European Radiology (2019) 29:1348–1354
https://doi.org/10.1007/s00330-018-5658-x

NEURO

MR imaging based fractal analysis for differentiating primary CNS lymphoma and glioblastoma

Shuai Liu[1,2] · Xing Fan[2] · Chuanbao Zhang[1] · Zheng Wang[1,2] · Shaowu Li[2,3] · Yinyan Wang[1] · Xiaoguang Qiu[4] · Tao Jiang[1,2,5]

Received: 20 October 2017 / Revised: 9 June 2018 / Accepted: 12 July 2018 / Published online: 30 August 2018

Abstract

Objectives The aim of this study was to differentiate primary central nervous system lymphoma (PCNSL) from glioblastomas (GBM) using the fractal analysis of conventional MRI data.

Materials and methods Sixty patients with PCNSL and 107 patients with GBM with MRI data available were enrolled. Fractal dimension (FD) and lacunarity values of the tumour region were calculated using fractal analysis. A predictive model combining fractal parameters and anatomical characteristics was built using logistic regression. The role of FD, lacunarity and the predictive model in differential diagnosis was evaluated using receiver-operating characteristic (ROC) curve analysis. The association between fractal parameters and anatomical characteristics of tumours was also investigated.

Results PCNSL had lower FD values ($p < 0.001$) and higher lacunarity values ($p < 0.001$) than GBM. ROC curve analysis revealed that FD, lacunarity, and the predictive model could distinguish PCNSL from GBM (area under the curve: 0.895, 0.776, and 0.969, respectively). The following associations were observed between fractal parameters and anatomical characteristics: multiple lesions were significantly associated with higher lacunarity ($p = 0.024$), necrosis with higher FD ($p = 0.027$), corpus callosum involvement with higher lacunarity ($p < 0.001$) in PCNSL and subventricular zone involvement with higher FD ($p < 0.001$) in GBM.

Conclusions The findings of the study indicate that fractal analysis on conventional MRI performs well in distinguishing PCNSL from GBM.

Key Points

- *Fractal dimension and lacunarity were capable of differentiating PCNSL from GBM.*
- *PCNSL and GBM exhibited different anatomical characteristics.*
- *Fractal parameters were associated with some of these anatomical characteristics.*

Keywords Lymphoma · Glioblastoma · Diagnosis · Magnetic resonance imaging · Fractals

✉ Xiaoguang Qiu
ttyy6611@sina.com

✉ Tao Jiang
taojiang1964@163.com

[1] Department of Neurosurgery, Beijing Tiantan Hospital, Capital Medical University, No. 6, Tiantan Xili, Dongcheng District, Beijing 100050, China

[2] Beijing Neurosurgical Institute, Capital Medical University, Beijing, China

[3] Department of Neuroradiology, Beijing Tiantan Hospital, Capital Medical University, Beijing, China

[4] Department of Radiation Oncology, Beijing Tiantan Hospital, Capital Medical University, No. 6, Tiantan Xili, Dongcheng District, Beijing 100050, China

[5] Center of Brain Tumor, Beijing Institute for Brain Disorders, Beijing, China

Abbreviations

AUC	Area under the curve
FD	Fractal dimension
GBM	Glioblastoma
MRI	Magnetic resonance imaging
PCNSL	Primary central nervous system lymphoma
ROC	Receiver operating characteristic
ROIs	Regions of interest

Introduction

Primary central nervous system lymphoma (PCNSL) and glioblastoma (GBM) are both highly malignant tumours of the central nervous system; however, they require completely

different treatment strategies. Surgery is recommended to alleviate symptoms and prevent recurrence in patients with GBM [1], but has no benefit in survival of patients with PCNSL [2]. Considering this stark difference in treatment, preoperative differentiation between these two diseases is important. Magnetic resonance imaging (MRI) is capable of non-invasive detection and assessment of brain tumours, which is recommended for all patients before treatment. However, differential diagnosis using routine conventional MRI is complicated because the images reveal significantly enhanced lesions surrounded by oedema in both PCNSL and GBM.

Because PCNSL and GBM exhibit similar appearances on post-contrast T1-weighted MRI, accurate differential diagnosis is difficult. However, PCNSL and GBM exhibit different cellularity, which may affect water diffusion in the interstitial space. Therefore, some studies have explored the usefulness of diffusion-weighted MRI sequences to differentiate PCNSL and GBM [3–5]. In addition, PCNSL and GBM exhibit different vascular permeability, perfusion and metabolic characteristics. Therefore, other studies have also evaluated the diagnostic value of perfusion imaging, including arterial spin labelling, and T1-weighted dynamic contrast-enhanced and dynamic susceptibility contrast-enhanced sequences [4–7], as well as molecular imaging, including endogenous protein-based amide proton transfer MRI [8] and positron emission tomography [4, 9]. However, despite great advances, these techniques are associated with increased time of examination and costs.

Fractal analysis is a promising tool for a neuroimaging study. It provides a method for quantitatively evaluating the texture and statistical properties of a shape or object [10]. Fractal dimension (FD) and lacunarity are parameters derived from fractal analysis; both are used to characterise fractal features. FD is used to describe the morphological complexity of an object [11]. An increased FD value indicates that an object is more irregular, which provides a quantitative index of roughness. Lacunarity is defined as the degree of gappiness, inhomogeneity or translational and rotational invariance. Higher lacunarity indicates greater heterogeneity and rotational variance [12]. These two parameters have been widely used in biology and medicine, especially in the analysis of central nervous system imaging data, such as those used to differentiate various brain tumours [13] and grade gliomas [14]. In this study, we aimed to differentiate between PCNSL and GBM by using fractal analysis of conventional MRI data. Our findings may elevate the power of conventional structural MRI imaging for differential diagnosis.

Materials and methods

Patients

Two cohorts of patients were retrospectively reviewed. Sixty patients with PCNSL treated at Beijing Tiantan Hospital (Beijing, China) between 2010 and 2014 were enrolled. Patients who met the following inclusion criteria were analysed: age > 18 years; histologically confirmed PCNSL; and available post-contrast T1-weighted MRI data of lesions before treatment. All PCNSL patients were immunocompetent. Data from 107 patients with GBM, diagnosed between 2010 and 2012, were collected from the database of the Chinese Glioma Genome Atlas. Inclusion criteria were as follows: age > 18 years; histologically confirmed de novo GBM; and available post-contrast T1-weighted MRI data of lesions before treatment. This retrospective study was approved by the Ethics Committee of Beijing Tiantan Hospital.

MRI protocol

MRI was mainly performed using a 3.0T MRI scanner (Siemens Trio, Siemens Healthcare, Erlangen, Germany). Post-contrast T1-weighted imaging (repetition time, 450 ms; echo time, 15 ms; section thickness, 5 mm) was performed with gadopentetate dimeglumine (Beilu Pharma) at a dose of 0.1 mmol/kg. The field of view was 240 × 240 mm^2 and the matrix size was 512 × 512.

Tumour segmentation and image normalisation

Tumour segmentation was performed using MRIcro software (http://www.mccauslandcenter.sc.edu/mricro/). Abnormal signals on post-contrast T1-weighted MRI were manually delineated as tumour regions of interest (ROIs) by a neurosurgeon (Fig. 1a). All ROIs were examined by a senior neuroradiologist (SWL) with 27 years of experience who was blinded to the clinical data of each patient. To reduce the influence of intensity differences, all MRI data were normalised using Matlab (R2014a, MathWorks, Natick, MA, USA) with an algorithm based on the studies by Nyúl et al [15] and Hellier et al [16].

Fractal analysis

Fractal analysis was performed using ImageJ software (U.S. National Institutes of Health, USA, http://imagej.nih.gov/ij/) and the built-in plugin Fraclac (Karperien-Charles Sturt University, Australia, https://imagej.nih.gov/ij/plugins/fraclac/FLHelp/Introduction.htm). ROIs of the tumours were extracted and loaded into Fraclac using its batch function. The box-counting method for grey-scale images was applied for fractal analysis (Fig. 1b). The box sizes within the grids were set from a minimum size of 1 pixel to a maximum size of 45% of the image dimension. Twelve grid positions were applied, and FD and lacunarity were calculated at each grid position to obtain mean values (i.e. FD and lacunarity values for each tumour slice were obtained). The mean FD and lacunarity values of all tumour slices in each patient were calculated

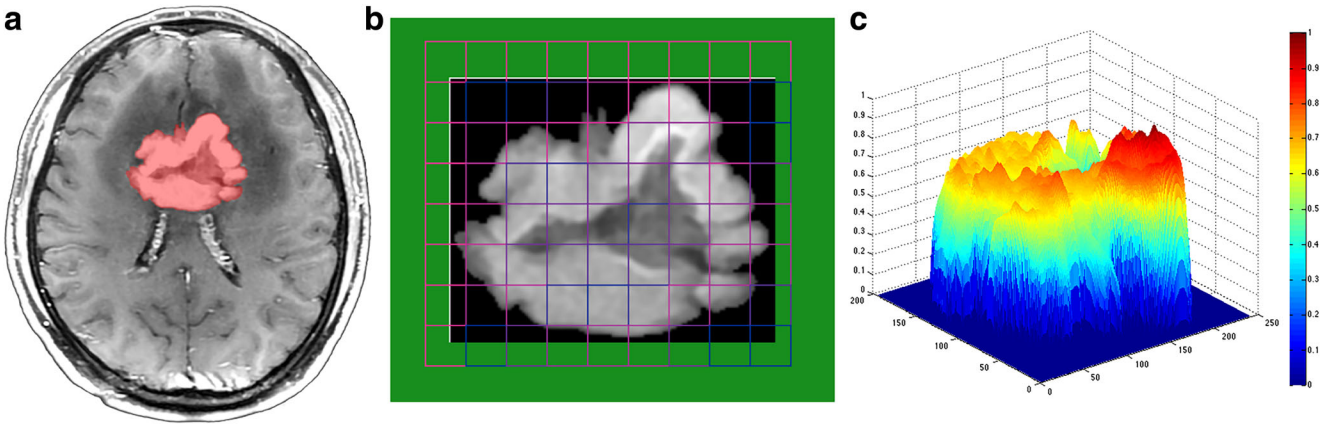

Fig. 1 The main process of image data processing. (**a**): Tumour segmentation. (**b**): Box-counting to grey-scale image of the tumour region is performed for fractal analysis. This method attempts to determine the average intensity of pixels per box. (**c**): Intensity map of the tumour region

and used in further analysis; more specifically, for patients with multiple lesions, the FD and lacunarity values were averaged for each lesion. For two patients with PCNSL with disseminated lesions, the largest lesions for fractal analysis were chosen using the above process.

Evaluation of anatomical characteristics

In both PCNSL and GBM groups, the number of lesions (single/multiple), tumour location (supratentorial/infratentorial), involvement of brain structures (central structures, cortex, subventricular zone and corpus callosum) and appearance of necrosis were evaluated. Specifically, the central structures listed above indicated the basal ganglia and thalamus. Further, the association of the anatomical characteristics and fractal parameters was investigated.

Statistical analysis

Statistical analysis was performed using R (https://www.r-project.org/) and several publicly available packages including ggplot2, pROC and plotROC. A chi-square test was performed to compare binary variables (Table 1). Student's t-test was used to compare FD and lacunarity values between the two diseases and different anatomical characteristics. Logistic regression was used to build the predictive model; $p < 0.05$ was considered to be statistically significant.

A predictive model combining fractal parameters and anatomical characteristics was built using logistic regression. FD, lacunarity, number of lesions, involvement of central structures and cortex, and presence of necrosis were entered into the logistic model, and factors with $p < 0.05$ were kept. A tenfold cross-validation was performed in the dataset.

Results

Clinical and MRI characteristics

In this study, 60 patients with PCNSL and 107 patients with GBM were enrolled. Both patient cohorts comprised a greater proportion of men (63% and 68%, respectively), with the

Table 1 Clinical and MRI characteristics of patients with PCNSL and GBM

MRI characteristic	PCNSL (%)	GBM (%)	*p*-value
Number	60	107	
Age, y (median, range)	54, 19-80	54, 18-77	0.372[2]
Male	38 (63)	73 (68)	0.609[1]
No. of lesions			**< 0.001**[1]
Single	41 (68)	104 (97)	
Multiple	19 (32)	3 (3)	
Localisation			
Only supratentorial	46 (76)	107 (100)	**< 0.001**[1]
Only infratentorial	7 (12)	0	
Supra- and infratentorial	7 (12)	0	
Involvement of brain structures			
Central structures[3]	31 (52)	4 (4)	**< 0.001**[1]
Cortex	11 (18)	68 (64)	**< 0.001**[1]
Subventricular zone	27 (45)	64 (60)	0.076[1]
Corpus callosum	9 (15)	17 (16)	1.000[1]
Appearance of necrosis	35 (58)	106 (99)	**< 0.001**[1]

MRI magnetic resonance imaging, *PCNSL* primary central nervous system lymphoma, *GBM* glioblastoma

[1] Chi-square test

[2] Student's t-test

[3] Basal ganglia and thalamus

The bold entries indicate as *p*-values < 0.05

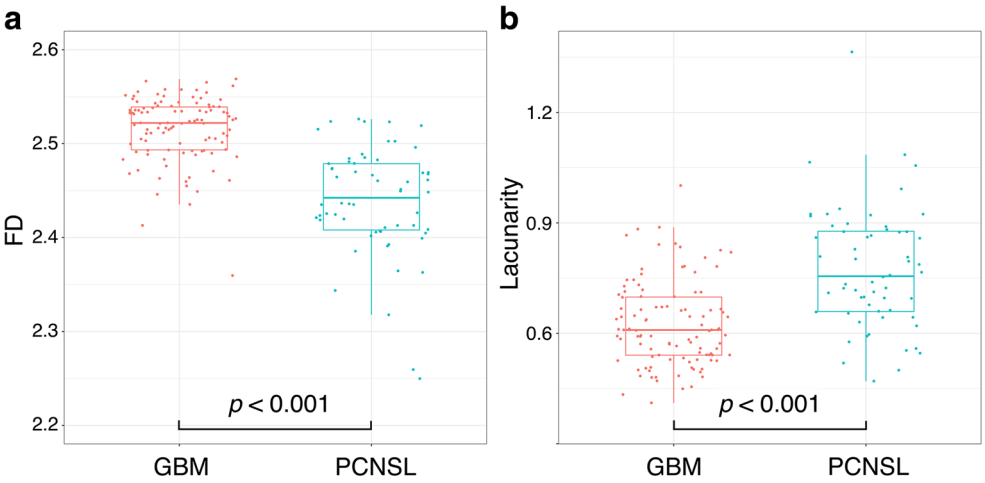

Fig. 2 Comparison between fractal dimension (FD) and lacunarity. Patients with primary central nervous system lymphoma (PCNSL) show a significantly lower FD value (**a**) and higher lacunarity value (**b**) than patients with glioblastoma (GBM)

same median age of 54 years. There were no significant differences in age or sex between the two cohorts.

The anatomical characteristics revealed on MRI indicated a higher number of patients with PCNSL had multiple lesions ($p < 0.001$), and tumours involving the central ($p < 0.001$) and infratentorial structures ($p < 0.001$), than patients with GBM. In contrast, more patients with GBM had tumours involving the brain cortex ($p < 0.001$) and presence of necrosis ($p < 0.001$). The detailed results are summarised in Table 1.

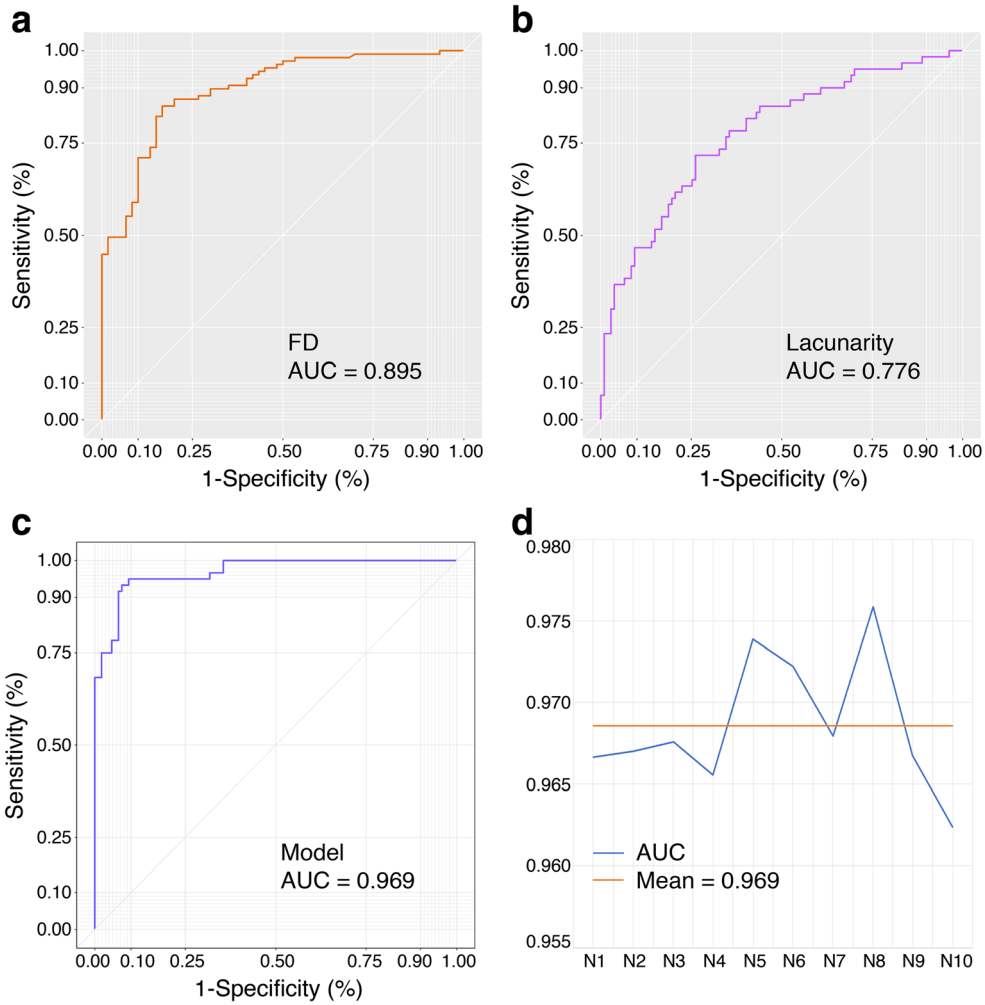

Fig. 3 Receiver-operating characteristic curve of fractal parameters and the predictive model are shown in a to c. Fractal dimension (FD) (**a**) demonstrates better performance than lacunarity (**b**) (area under the curve [AUC]: 0.895 vs. 0.776, respectively). The AUC of the predictive model was 0.969 (**c**). The AUCs of the tenfold validation (from N1 to N10) (**d**) are shown with the blue line, and the average of the AUCs is shown with the red line

Characteristics and predictive role of fractal parameters

Significant differences in FD and lacunarity were found between the PCNSL and GBM groups. Specifically, patients with PCNSL had lower FD ($p < 0.001$) and higher lacunarity ($p < 0.001$) values than patients with GBM (Fig. 2a and b).

Receiver-operating characteristic (ROC) curve analysis demonstrated that PCNSL could be distinguished from GBM using fractal parameters. The area under the curve (AUC) of FD was 0.895 (95% confidence interval [CI]: 0.847–0.943) (Fig. 3a), and the sensitivity and specificity were 0.851 and 0.833, respectively. For lacunarity, the AUC was 0.776 (95% CI: 0.702–0.851) (Fig. 3b), and the sensitivity and specificity were 0.717 and 0.738, respectively.

After logistic regression, FD, lacunarity, involvement of central structures and presence of necrosis were kept in the predictive model. The AUC of the model was 0.969 (95% CI: 0.945–0.992) (Fig. 3c), and the sensitivity and specificity were 0.933 and 0.925, respectively. The details of the tenfold validation are shown in Fig. 4d, and the average of the AUCs was 0.969.

Relationship between the fractal parameters and anatomical findings

The lacunarity value of PCNSL with multiple lesions was significantly higher than that of tumours with a single lesion ($p = 0.024$; Fig. 4a). GBM involving the subventricular zone had a significantly higher FD value than tumours that did not involve this zone ($p < 0.001$) (Fig. 4b). In PCNSL, tumours that involved the corpus callosum had significantly higher lacunarity values than tumours that did not involve the corpus callosum ($p < 0.001$) (Fig. 4c), and tumours with necrosis had significantly higher FD values than tumours without necrosis ($p = 0.027$) (Fig. 4d).

Discussion

In the current study, we performed fractal analysis on conventional MRI data of two separate cohorts consisting of patients with PCNSL and patients with GBM. The FD value demonstrated promising performance in the differential diagnosis of

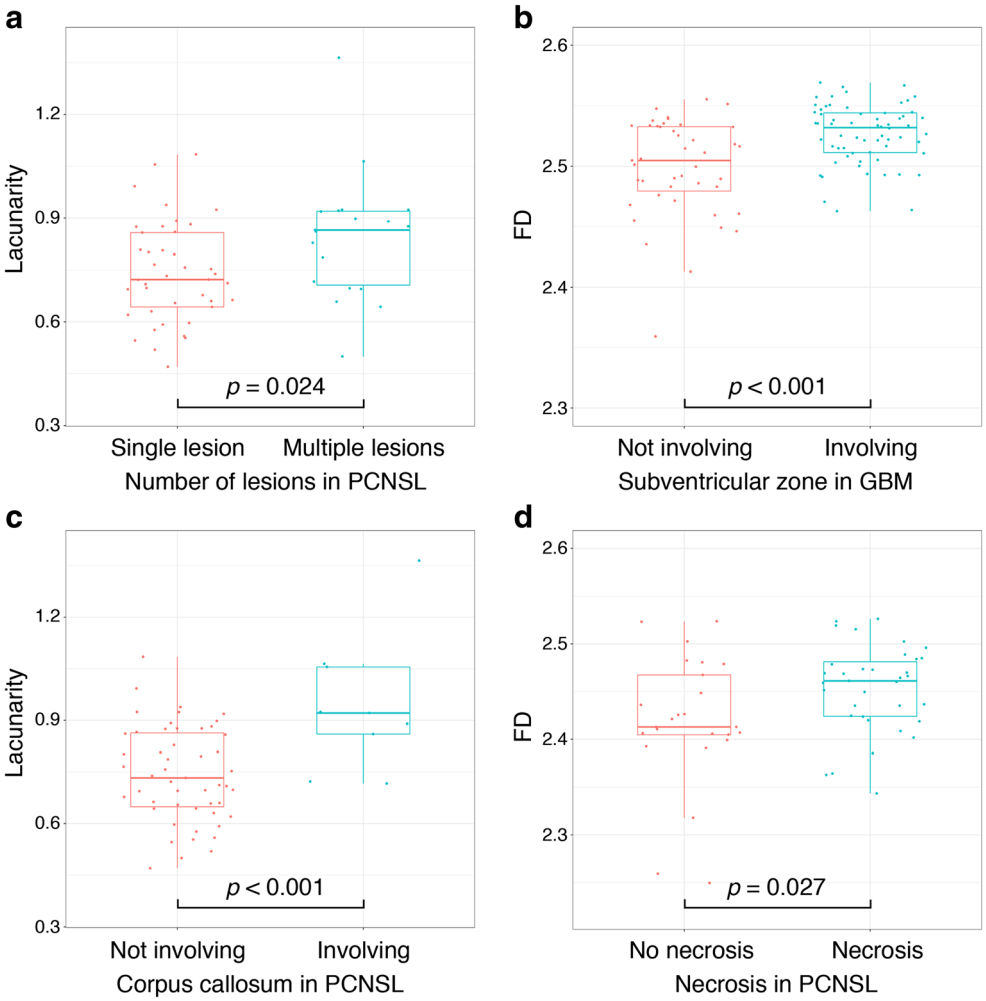

Fig. 4 The association between fractal parameters and anatomical characteristics. (**a**): Comparison of lacunarity value according to the number of lesions in primary central nervous system lymphoma (PCNSL); (**b**) comparison of fractal dimension (FD) value according to tumours involving the subventricular zone (or not) in glioblastoma (GBM); (**c**) comparison of lacunarity value according to tumours involving the corpus callosum (or not) in PCNSL; (**d**) comparison of FD value according to tumours with necrosis (or not) in PCNSL

these two diseases. We further built a multivariate predictive model including fractal parameters and anatomical characteristics of the tumours. This model showed high power to differentiate PCNSL and GBM. In addition, we observed an association between fractal parameters and anatomical characteristics in both PCNSL and GBM.

Fractal analysis is a promising tool for evaluating texture characteristics on MRI. This method has been widely used to evaluate the complexity of pathological patterns [17]. As MRI is a manifestation of a tumour's microstructure, fractal features could be used to evaluate the biological properties of PCNSL and GBM. Studies investigating cancer using imaging data revealed that FD could be used for differential diagnosis [13, 14, 18] and efficacy evaluation [19–21]. In the current study, we found that the FD value of GBM was significantly higher than that of PCNSL. Moreover, FD demonstrated good predictive values for the differential diagnosis between PCNSL and GBM. These findings suggest that GBM exhibits a more complicated texture pattern on MRI than PCNSL, which is consistent with the heterogeneous nature of GBM [22, 23].

In some cases, an image yields the same FD values but strikingly different texture(s), which can be described by lacunarity. Lacunarity has also been widely used in processing medical images [14, 24, 25]. As mentioned above, PCNSL had lower FD values than GBM, but had higher lacunarity values. Necrosis is primarily visualised as gaps in the tumour lesion and is always localised in the centre of the tumour; this positioning may reduce its rotational variance. In addition, we used the box-counting method for grey-scale images. Compared with binary images, regions of necrosis are not simply recognised as a blank area. The enhancement patterns on MRI also affected the lacunarity value.

Advanced neuroimaging techniques such as diffusion and perfusion MRI as well as molecular imaging have been used to differentiate PCNSL and GBM [3–7]. In those studies, the AUCs of the parameters ranged from 0.680 to 0.963. In the current study, we analysed data acquired from conventional MRI, which is essential and more convenient in clinical practice. The AUCs of FD and lacunarity were 0.895 and 0.776, respectively, and the AUC of the predictive model reached 0.969. These results were robust and practicable. In addition, the number of patients was significantly larger than in the previously cited studies, which contributes to strengthening, if not validating, our results.

On comparing the anatomical characteristics revealed by conventional MRI, some significant differences between PCNSL and GBM were demonstrated. Necrosis is a hallmark feature of GBM and, accordingly, we found necrosis in nearly all GBM cases (99%). In contrast, necrosis was observed in only 58% of PCNSL cases. Although this percentage was significantly lower than that of GBM, it was higher than that reported in other studies [26–28]. In particular, we found that tumours exhibiting necrosis had significantly higher FD values in PCNSL. GBMs located in the infratentorial area or with multiple lesions are rare [29]. However, infratentorial or multifocal PCNSLs were more commonly observed in the present study, which is consistent with previous findings [30]. Interestingly, PCNSLs with multiple lesions demonstrated higher lacunarity values than single-lesion tumours. These findings illustrate the differences in anatomical characteristics between PCNSL and GBM, and that some of these characteristics are associated with fractal parameters.

Several limitations should be considered in this study. There are several algorithms for fractal analysis, including the modified box-counting method using linear discriminant analysis and the modified Minkowski method [31]. The fractal dimension calculated by these algorithms could be slightly discordant. In addition, there is no standard method of fractal analysis for different image properties and study purposes. In this study, we performed fractal analysis by using Fraclac, a free-access software program. It provides an easier way to perform fractal analysis and reproduce studies. Further, two fractal parameters including fractal dimension and lacunarity were obtained by this method, which could better describe the results of fractal analysis. Tumour segmentation is another important issue for imaging studies. Compared to T1 and T2 sequences, T1-enhanced sequences can better exhibit the boundary of PCNSL and GBM (not the biological boundary). Despite the development of automatic segmentation techniques, manual segmentation of brain tumours is still considered to be more reliable. In this study, the ROIs were drawn by a neurosurgeon who focuses on neuroimaging studies of brain tumours. To minimise inaccuracy, these ROIs were further checked by a senior neuroradiologist (27 years of experience).

In summary, we compared the general and fractal characteristics of conventional MRI findings between PCNSL and GBM. Significant differences in anatomical locations and fractal parameters, including FD and lacunarity, were observed. In particular, we found that FD alone and the predictive model demonstrated favourable performance in the differential diagnosis of PCNSL and GBM, and fractal parameters showed an association with the anatomical characteristics of the tumours. These findings will help increase the differential diagnostic yield of routine conventional MRI.

Funding This study has received funding by the Capital Medical Development Research Fund (2016-2-1073), the National Key Research and Development Plan (No. 2016YFC0902500) and the Beijing Postdoctoral Research Foundation (2017-ZZ-116).

Compliance with ethical standards

Guarantor The scientific guarantor of this publication is Tao Jiang.

Conflict of interest The authors of this manuscript declare no relationships with any companies whose products or services may be related to the subject matter of the article.

Statistics and biometry No complex statistical methods were necessary for this paper.

Informed consent Written informed consent was obtained from all subjects (patients) in this study.

Ethical approval Institutional Review Board approval was obtained.

Methodology
- Retrospective
- Diagnostic or prognostic study
- Performed at one institution

References

1. Weller M, van den Bent M, Tonn JC et al (2017) European Association for Neuro-Oncology (EANO) guideline on the diagnosis and treatment of adult astrocytic and oligodendroglial gliomas. Lancet Oncol. https://doi.org/10.1016/S1470-2045(17)30194-8
2. Hoang-Xuan K, Bessell E, Bromberg J et al (2015) Diagnosis and treatment of primary CNS lymphoma in immunocompetent patients: guidelines from the European Association for Neuro-Oncology. Lancet Oncol 16:e322–e332
3. Wang S, Kim S, Chawla S et al (2011) Differentiation between glioblastomas, solitary brain metastases, and primary cerebral lymphomas using diffusion tensor and dynamic susceptibility contrast-enhanced MR imaging. AJNR Am J Neuroradiol 32:507–514
4. Yamashita K, Yoshiura T, Hiwatashi A et al (2013) Differentiating primary CNS lymphoma from glioblastoma multiforme: assessment using arterial spin labeling, diffusion-weighted imaging, and (1)(8)F-fluorodeoxyglucose positron emission tomography. Neuroradiology 55:135–143
5. Lin X, Lee M, Buck O et al (2017) Diagnostic Accuracy of T1-Weighted Dynamic Contrast-Enhanced-MRI and DWI-ADC for Differentiation of Glioblastoma and Primary CNS Lymphoma. AJNR Am J Neuroradiol 38:485–491
6. Kickingereder P, Sahm F, Wiestler B et al (2014) Evaluation of microvascular permeability with dynamic contrast-enhanced MRI for the differentiation of primary CNS lymphoma and glioblastoma: radiologic-pathologic correlation. AJNR Am J Neuroradiol 35: 1503–1508
7. Nakajima S, Okada T, Yamamoto A et al (2015) Differentiation between primary central nervous system lymphoma and glioblastoma: a comparative study of parameters derived from dynamic susceptibility contrast-enhanced perfusion-weighted MRI. Clin Radiol 70:1393–1399
8. Jiang S, Yu H, Wang X et al (2016) Molecular MRI differentiation between primary central nervous system lymphomas and high-grade gliomas using endogenous protein-based amide proton transfer MR imaging at 3 Tesla. Eur Radiol 26:64–71
9. Okada Y, Nihashi T, Fujii M et al (2012) Differentiation of newly diagnosed glioblastoma multiforme and intracranial diffuse large B-cell Lymphoma using (11)C-methionine and (18)F-FDG PET. Clin Nucl Med 37:843–849
10. Lennon FE, Cianci GC, Cipriani NA et al (2015) Lung cancer-a fractal viewpoint. Nat Rev Clin Oncol 12:664–675
11. Fernandez E, Jelinek HF (2001) Use of fractal theory in neuroscience: methods, advantages, and potential problems. Methods 24: 309–321
12. Plotnick RE, Gardner RH, O'Neill RV (1993) Lacunarity indices as measures of landscape texture. Landscape ecology 8:201–211
13. Di Ieva A, Le Reste PJ, Carsin-Nicol B, Ferre JC, Cusimano MD (2016) Diagnostic Value of Fractal Analysis for the Differentiation of Brain Tumors Using 3-Tesla Magnetic Resonance Susceptibility-Weighted Imaging. Neurosurgery 79:839–846
14. Smitha KA, Gupta AK, Jayasree RS (2015) Fractal analysis: fractal dimension and lacunarity from MR images for differentiating the grades of glioma. Phys Med Biol 60:6937–6947
15. Nyúl LG, Udupa JK (1999) On standardizing the MR image intensity scale. Magn Reson Med 42:1072–1081
16. Hellier P (2003) Consistent intensity correction of MR imagesImage Processing, 2003 ICIP 2003 Proceedings 2003 International Conference on. IEEE, pp I-1109
17. Cross SS (1997) Fractals in pathology. J Pathol 182:1–8
18. Miwa K, Inubushi M, Wagatsuma K et al (2014) FDG uptake heterogeneity evaluated by fractal analysis improves the differential diagnosis of pulmonary nodules. Eur J Radiol 83:715–719
19. Hayano K, Yoshida H, Zhu AX, Sahani DV (2014) Fractal analysis of contrast-enhanced CT images to predict survival of patients with hepatocellular carcinoma treated with sunitinib. Dig Dis Sci 59: 1996–2003
20. Hayano K, Lee SH, Yoshida H, Zhu AX, Sahani DV (2014) Fractal analysis of CT perfusion images for evaluation of antiangiogenic treatment and survival in hepatocellular carcinoma. Acad Radiol 21:654–660
21. Breki CM, Dimitrakopoulou-Strauss A, Hassel J et al (2016) Fractal and multifractal analysis of PET/CT images of metastatic melanoma before and after treatment with ipilimumab. EJNMMI Res 6:61
22. Cha S (2006) Update on brain tumor imaging: from anatomy to physiology. AJNR Am J Neuroradiol 27:475–487
23. Inda MM, Bonavia R, Seoane J (2014) Glioblastoma multiforme: a look inside its heterogeneous nature. Cancers (Basel) 6:226–239
24. Yasar F, Akgünlü F (2005) Fractal dimension and lacunarity analysis of dental radiographs. Dentomaxillofac Radiol 34:261–267
25. Karperien A, Jelinek H, Milosevic N (2011) Reviewing lacunarity analysis and classification of microglia in neuroscience. 8th European Conference on Mathematical and Theoretical Biology, Poland
26. Haldorsen IS, Kråkenes J, Krossnes BK, Mella O, Espeland A (2009) CT and MR imaging features of primary central nervous system lymphoma in Norway, 1989-2003. AJNR Am J Neuroradiol 30:744–751
27. Küker W, Nägele T, Korfel A et al (2005) Primary central nervous system lymphomas (PCNSL): MRI features at presentation in 100 patients. J Neurooncol 72:169–177
28. Malikova H, Koubska E, Weichet J et al (2016) Can morphological MRI differentiate between primary central nervous system lymphoma and glioblastoma? Cancer Imaging 16:40
29. Larjavaara S, Mäntylä R, Salminen T et al (2007) Incidence of gliomas by anatomic location. Neuro Oncol 9:319–325
30. Rubenstein J, Ferreri AJ, Pittaluga S (2008) Primary lymphoma of the central nervous system: epidemiology, pathology and current approaches to diagnosis, prognosis and treatment. Leuk Lymphoma 49(Suppl 1):43–51
31. Li H, Giger ML, Olopade OI, Lan L (2007) Fractal analysis of mammographic parenchymal patterns in breast cancer risk assessment. Acad Radiol 14:513–521